Modulating Energy Among Foot-Ankle Complex With an Unpowered Exoskeleton Improves Human Walking Economy

Di Hu, Caihua Xiong, *Member, IEEE*, Tao Wang, Tiancheng Zhou, Jiejunyi Liang, and Yuhao Li

***Abstract*— Over the course of both evolution and development, the human musculoskeletal system has been well shaped for the cushion function of the foot during foot-strike and the impulsive function of the ankle joint during push-off. Nevertheless, an efficient energy interaction between foot structure and ankle joint is still lacking in the human body itself, which may limit the further potential of economical walking. Here we showed the metabolic expenditure of walking can be lessened by an unpowered exoskeleton robot that modulates energy among the foot-ankle complex towards a more effective direction. The unpowered exoskeleton recycles negative mechanical energy of the foot that is normally dissipated in heel-strike, retains the stored energy before mid-stance, and then transfers the energy to the ankle joint to assist the push-off. The modulation process of the exoskeleton consumes no input energy, yet reduces the metabolic cost of walking by 8.19 $\pm$ 0.96 % (mean $\pm$ s.e.m) for healthy subjects. The electromyography measurements demonstrate the activities of target ankle plantarflexors decreased significantly without added effort for the antagonistic muscle, suggesting the exoskeleton enhanced the subjects' energy efficiency of the foot-ankle complex in a natural manner. Furthermore, the exoskeleton also provides cushion assistance for walking, which leads to significantly decreased activity of the quadriceps muscle during heel-strike. Rather than strengthening the functions of existing biological structures, developing the complementary energy loop that does not exist in the human body itself also shows its potential for gait assistance.**

***Index Terms*— Human walking, metabolic cost reduction, wearable robotics, foot-ankle biomechanics, human response, energetics.**

Manuscript received 1 March 2022; revised 7 May 2022 and 12 June 2022; accepted 29 June 2022. Date of publication 6 July 2022; date of current version 20 July 2022. This work was supported in part by the National Natural Science Foundation of China under Grant 52027806, Grant U1913601, Grant 52005191, Grant 52075191, and Grant U1913205; in part by the National Key Research and Development Program under Grant 2020YFC2007802; and in part by the Hubei Provincial Natural Science Foundation under Grant 2020CFB424. *(Corresponding author: Caihua Xiong.)*

This work involved human subjects or animals in its research. Approval of all ethical and experimental procedures and protocols was granted by the Chinese Ethics Committee of Registering Clinical Trials under Application No. ChiECRCT20200232.

The authors are with the State Key Laboratory of Digital Manufacturing Equipment and Technology, Institute of Rehabilitation and Medical Robotics, Huazhong University of Science and Technology, Wuhan, Hubei 430074, China (e-mail: chxiong@hust.edu.cn).

This article has supplementary downloadable material available at https://doi.org/10.1109/TNSRE.2022.3188870, provided by the authors.

Digital Object Identifier 10.1109/TNSRE.2022.3188870

I. Introduction

WALKING is one of the most common and essential activities in human daily life. The gait of human walking results from energy generation, absorption, and transfer among the body's segments [1], [2]. Being the extreme part of the leg to directly interact with the ground, the foot-ankle complex plays an essential role in both energy absorption and energy generation during walking. During the early stance of walking gait, the foot functions as a compliant structure and absorbs energy to cushion the collision as the foot strikes the ground [3], [4]. In the late stance, the ankle joint produces a larger burst of work than any other joint, helping the forward propulsion during push-off [5]–[7]. Such a well-shaped foot-ankle musculoskeletal system for walking is the result of both the evolution and development process [8]–[10]. Nevertheless, in each step of walking, considerable energy is still required for ankle push-off while foot-strike dissipates substantial energy. Modulating biomechanical energy among foot-ankle complex to make walking more efficient is consequently an intriguing research topic. Given the inherent factors of anatomical and physiological structures are difficult to adjust, researchers have been making attempts to modulate energy and augment walking performance using wearable assistive devices of exoskeletons [11]–[13].

Over the last decade, great progress has been made in modulating energy within the ankle joint by employing exoskeletons to enhance the walking economy [14]. Some exoskeletons are powered and intended to use the mechanical work done by actuators to replace the biomechanical work performed by ankle muscles. Based on this principle, several portable exoskeletons were successfully designed to reduce the metabolic cost of walking versus without the exoskeleton [15]–[17]. In addition, tethered-powered exoskeletons also made advancements in seeking optimized assistive strategies for the ankle joint to further reduce the metabolic cost of walking [18]–[20]. While the powered exoskeleton can provide biologically appropriate levels of mechanical power, larger assisting magnitude and longer assisting duration require batteries and actuators with increasing mass, which result in added metabolic burden. Hence, researchers have to make a trade-off between the assisting capability and the mass penalty caused by the batteries and actuators [12], [21]. Alternatively, the unpowered exoskeletons utilize passive mechanical elements such as springs and clutches to recycle energy and

improve the overall energy efficiency during walking. The first successful attempt of unpowered exoskeletons recycled energy during ankle dorsiflexion to assist the following ankle push-off and utilized a passive mechanical clutch to mimic the isometric contraction of calf muscles [22]. Nevertheless, human-in-the-loop optimizations using tethered powered exoskeletons have demonstrated applying higher ankle assistive moment with net energy input during late stance can further improve the walking economy [19], [20]. Therefore, seeking an energy source outside of the ankle joint may be more beneficial for walking assistance.

Recently, advancements have been made in using the knee and hip joints as energy sources given their considerable magnitudes of negative joint works [23]–[25]. However, co-contractions of antagonistic muscles have been found to counteract the assistive moment when storing energy from joint motions with negative powers, which could partly offset the assisting capability of unpowered exoskeletons [22], [26]. Except for lower limb joints, recent biomechanical studies revealed the structures beneath the hindfoot also absorb substantial energy when the foot strikes the ground in the early stance of walking [4], [27]. Different from the joint motions, the strike motion between foot and substrate has no specific antagonistic muscles. The foot-strike is consequently a promising energy source for unpowered exoskeletons that may circumvent the metabolic penalty caused by antagonistic co-contraction. In fact, previous studies [28], [29] have shown the feasibility of recycling foot-strike energy using quasi-passive prothesis feet to restore the impaired walking capability of amputees. In the case of normal walking of healthy people, the structures responsible for the energy absorption during the foot-strike include the biological tissue of the heel pad and the rearfoot region of footwear [27], which were previously related to protecting the human body from strike-induced injuries [30], [31]. Besides, the recent biomechanical study about foot and ankle found they collectively resembled an energy-neutral system that performed small work on environment [32], which also indicated the possibility of recycling energy among foot-ankle complex with no energy input, and ultimately reducing the metabolic cost of walking.

Despite these promising evidences, how to effectively modulate energy among the foot-ankle complex during normal walking by unpowered exoskeleton remains challenging. While the beneath-hindfoot structures are potential sources to store energy for unpowered exoskeletons, they may not be appropriate places to release energy for assisting walking. It is because the beneath-hindfoot structures primarily absorb and dissipate energy and little energy input is required during walking [24], [31]. By contrast, the ankle joint is one of the body's major energy generators during walking, especially during push-off [5]. The ankle joint is thus a proper assistive target to release the stored energy for providing walking assistance. Moreover, the timing and manner of releasing energy to the ankle joint are also essential to efficient walking. For instance, the impulsive force of ankle plantarflexors during the late stance phase contributes substantially to supporting body weight and powering leg swing during walking [6], [33]. Therefore, when formulating the energy modulation strategy, we should not only pay attention to the energy transfer between foot and ankle, but also attach importance to the timing and manner of collecting and releasing energy. These functional complexities also pose challenges to the physical implementation of the unpowered exoskeleton.

In this study, we first analyzed the power/energy profiles of the ankle joint and beneath-hindfoot structure to ratiocinate a phased energy modulation strategy for the improved walking economy. Then we developed an unpowered exoskeleton with a series-parallel hybrid configuration to realize the energy modulation among the foot-ankle complex (Fig. 1). Specifically, the exoskeleton applied a series-hindfoot mechanism to recycle the foot-strike energy during the heel-strike phase. After retaining the stored energy during the early and middle stance phase, the parallel-ankle mechanism was used to further store energy from late dorsiflexion of the ankle joint, then release the entire stored energy to assist ankle plantarflexion during the push-off phase. Torsion springs were used as energy storage containers, while passive mechanical clutches were designed to control the timing of energy recycling, retaining, and releasing. To study the applicability of the presented energy modulation strategy for metabolic cost reduction, the designed exoskeleton was tested on eight health subjects in walking experiments at 1.25 m/s. In addition to net metabolic rate, we also measured and statistically analyzed lower limb muscle activities, joint kinematics, joint kinetics, and exoskeleton mechanics to further study the human responses to the proposed energy modulation strategy. For evaluating the biomechanical influences of the assistance magnitude of the energy modulation strategy, the experiments were performed across different exoskeleton assistance conditions. Through these analyses, we hope our study can not only realize an efficient energy modulation between foot and ankle, but also give a deeper understanding of the energetics and biomechanics of human walking.

II. Materials and Methods

A. Reasoning of Energy Modulation Strategy

The energy modulation strategy is based on the energy analysis of the foot-ankle complex during human walking. As mentioned above, ankle joint and foot structures generally play different roles: the ankle joint is characterized by performing a burst of positive work and thus requires energy input, while the foot structures primarily dissipate energy [32], [34]. Among the structures contributing to energy dissipation distal to the foot, the soft tissues beneath the hindfoot are suitable to recycle energy due to their purely damping function and having no specific antagonistic muscles. Hence, our energy analyses about the foot-ankle complex focused on not only the ankle power but also the beneath-hindfoot power.

As human walking is a periodic motion, we analyzed the foot and ankle power characteristics in a gait cycle (Fig. 1f). The beneath-hindfoot power typically exhibits negative values as the foot strike the ground between 0-15% of the gait cycle, defined as the early stance phase. In contrast, the power profile of the ankle joint during a gait cycle comprises a long period with low negative power, followed by a short period with high positive power. The negative power period of the ankle joint exhibits near-zero power values at the initial period, and then sharply becomes high at around 30% of the gait cycle.

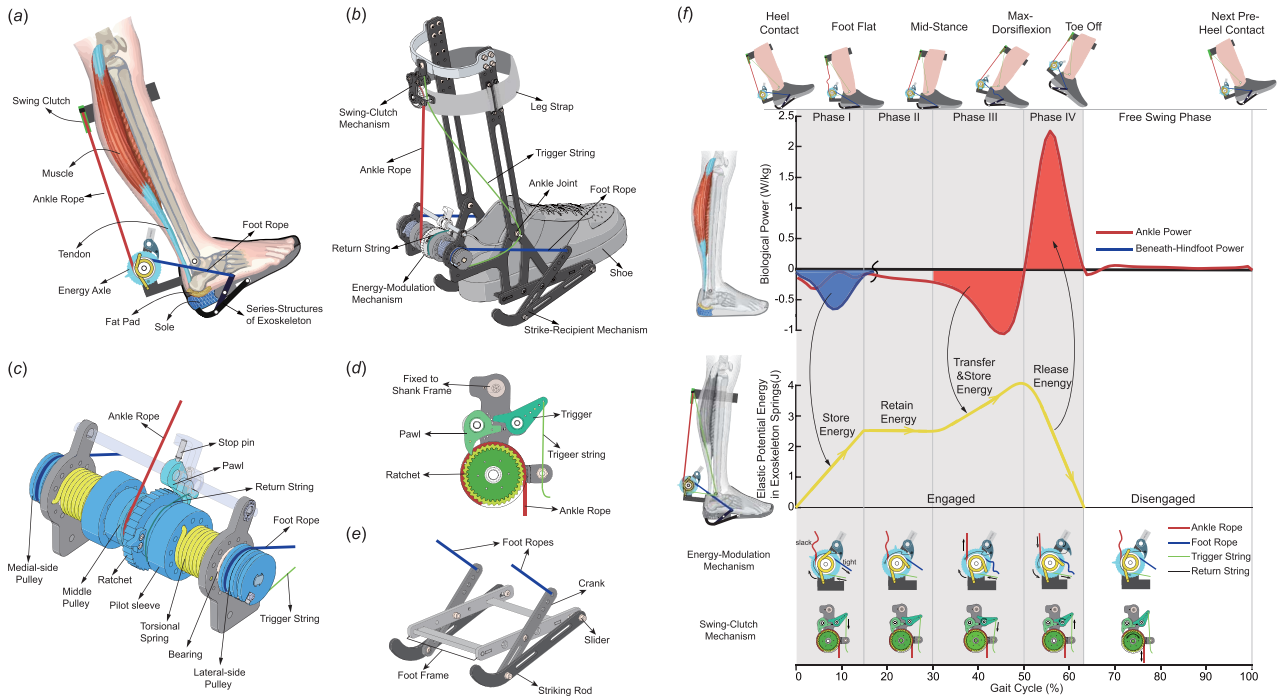

Fig. 1. Unpowered foot-ankle exoskeleton design. (a) Schematic design showing the series-parallel hybrid configuration of the unpowered foot-ankle exoskeleton. (b) Mechanical structure of the unpowered foot-ankle exoskeleton. (c) and (d) Enlarged views for the energy-modulation mechanism, the swing-clutch mechanism and the strike-recipient mechanism. (e) Principle scheme showing the energy modulation strategy and working process of the unpowered foot-ankle exoskeleton. (f) Energy modulation strategy and working process of the unpowered foot-ankle exoskeleton.

The positive power period of the ankle joint begins as the ankle reaches maximum dorsiflexion at around 50% of the gait cycle, and ends as the foot leaves the ground at around 63% of the gait cycle. Putting the profiles of ankle joint power and beneath-hindfoot power together, there are two obvious intervals that both power's values are near zero. One is the period between 15% to 30% of the gait cycle. The other interval is between 63% to 100% of the gait cycle, defined as the swing phase that the foot leaves the ground and the leg is swung in the air.

According to the above power analysis in a gait cycle, we proposed a periodically-phased strategy to modulate energy among the foot-ankle complex for enhanced overall energy efficiency (Fig. 1f). To be specific, during the early stance phase (0-15% of the gait cycle, phase I), the negative power of the foot-strike is stored by the exoskeleton. Such energy storage not only reduces the energy dissipation during foot-strike but also has the potential to reduce the metabolic cost of cushion [35]. Then the stored energy should be retained in the exoskeleton before the middle stance (15-30% of gait cycle, phase II). As the ankle joint continues to dorsiflex with increasing negative power (30%-50% of gait cycle, phase III), the exoskeleton continues to store energy from the ankle joint and provides assisting plantarflexion moment. After the ankle joint reaches the maximum dorsiflexion, the stored energy is then all released to the ankle joint to assist its plantarflexion (50%-63% of gait cycle, phase IV), which likely reduces the positive work produced by the ankle plantarflexor. Finally, the natural motions of the foot and ankle should not be disturbed during the swing phase (63%-100% of the gait cycle). In all, the proposed energy modulation strategy is anticipated to provide humans with a complementary loop that passively recycles and transfers biomechanical energy among the foot-ankle complex in an energy-effective way.

B. Design of the Unpowered Exoskeleton

To realize the presented idea for energy modulation among the foot-ankle complex, we designed a lightweight unpowered exoskeleton with passive mechanisms placed in a series-parallel hybrid configuration. As depicted in Fig. 1a-e, the key aspects of our exoskeleton design include: (i) two conformal frame elements fixed to shank and foot respectively, which are connected with an artificial ankle joint, (ii) a compact slider-crank mechanism distal to foot frame to reify the deformation of the beneath-hindfoot structure during foot-strike (the strike-recipient mechanism), (iii) an intermittent motion mechanism in parallel with foot frame to enable energy modulation among foot and ankle joint during stance phase (the energy-modulation mechanism), and (iv) a ratchet-pawl-trigger mechanism located in parallel with shank frame to allow free motion of ankle joint during swing phase (the swing-clutch mechanism). These sets of components are elaborately designed to work together to recycle, store, retain and release energy at the proper time in each gait cycle of walking, as elucidated as follows.

The energy containers used in our exoskeleton are torsional springs, whose two ends are fixed to the energy axle of the energy-modulation mechanism and foot frame. Consequently, the positive rotation of the energy axle leads to the twist of assistive torsional springs and energy storage, while the negative rotation of the energy axle is accompanied by the recovery of torsional springs and energy release. Except for the pilot

sleeves used as fixed bases of torsional springs, the energy axle also involves two side pulleys, a middle pulley, a ratchet with a release arm, and a return arm. The side pulleys are connected to the cranks of the strike-recipient mechanism by means of two ropes (foot ropes). Using foot ropes, the foot-strike deformation drives the energy axle and twists torsional springs in the positive direction to store energy during the early-stance phase (0-15% of the gait cycle). The ratchet is meshed with the pawl before the mid-stance phase (0-30% of the gait cycle) to prevent negative rotation of the energy axle so that the stored energy can be retained without extra efforts from the human. Besides, another rope (ankle rope) is connected from the middle pulley to the shank segment to transfer energy and exert moment on the ankle joint. The ankle rope is set to be initially tight around the beginning of the late-stance phase (30% of the gait cycle). In this way, the ankle rope is slack before the mid-stance phase (0-30% of the gait cycle), and tight during the late stance phase (30%-63% of the gait cycle). From 30% of the gait cycle to the maximum dorsiflexion position of the ankle joint, the ankle dorsiflexion motion drives the energy axle in the positive direction using ankle rope. On the one hand, with the positive rotation of the energy axle, the release arm pushes the pawl away from the ratchet, enabling the stored energy to transfer to the ankle joint. On the other hand, the positive rotation of the energy axle twists torsional springs to further store energy during ankle dorsiflexion. From the maximum dorsiflexion position of the ankle joint to toe-off (63% of the gait cycle), the recovery of the torsional spring rotates the energy axle negatively. Meanwhile, all stored energy is released to assist ankle plantarflexion. With the energy axle returning to the rest position at toe-off (63% of the gait cycle), the return arm pulls the pawl back to be meshed with the ratchet through a fibrous return string.

After modulating energy among the foot-ankle complex during the stance phase of gait, the exoskeleton should avoid disturbing natural ankle movement during leg swing. Thus, we developed a free-motion mechanism to engage a clutch to link the shank segment with the energy-modulation mechanism when the foot is on the ground and disengage this clutch to allow free motion when the foot is swung in the air. Inspired by the traditional ratchet-pawl clutch and previous works [22], [25], we designed a ratchet-pawl-trigger mechanism for the clutching function. The rotation of the energy axle of the energy-modulation mechanism is used as a robust trigger signal for the engagement of the clutch, since the energy axle only rotates during the stance phase and is always motionless in the rest position during the swing phase. Specifically, a trigger string is connected between the energy axle of the energy-modulation mechanism and the trigger of the swing-clutch mechanism. The trigger string is threaded through the ankle joint to avoid the influence of ankle motion on the trigger. As the trigger is fired by foot striking the ground, a small coil spring in the pawl will engage the pawl with the ratchet. Meanwhile, the small coil spring in the ratchet resets the ratchet and adjusts the ankle rope to be an appropriate length, so that the ankle rope can be initially tight at the beginning of the late-stance phase (30% of the gait cycle). Throughout the late-stance phase (30%-63% of the gait cycle), the clutch is engaged and the ankle rope is tight to exert moment on the ankle joint. Once the foot leaves the ground, the energy axle of the energy-modulation mechanism and the trigger of the swing-clutch mechanism return to their rest positions, leading to the disengagement of the clutch. Subsequently, the ankle joint can move freely until the heel-strike of the next gait cycle. The working process of the exoskeleton during walking is illustrated in Fig. 2. In addition, the demonstration of the subject walking during exoskeleton assistance experiment was provided in the Supplementary Video.

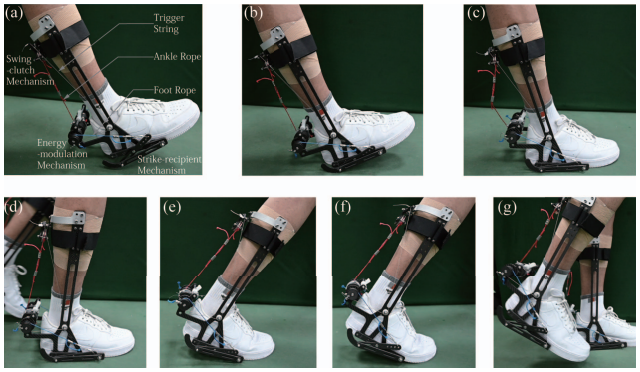

Fig. 2. Subject walking with the unpowered foot-ankle exoskeleton. (a). Before heel-contact. (b) Heel-contact. (c) Foot-flat. (d) Mid-stance. (e) Max-dorsiflexion. (f) Push-off. (g) Swing phase.

The total weight of our exoskeleton is 655 g for one side, and the detailed mass distribution is presented in Supplementary Table S1. The assistive torsional spring can be interchanged with different stiffness for different modulation magnitudes. The more detailed specifications and parameter design criteria about our exoskeleton were presented in Supplementary Note S1 and Note S2 separately. In addition, the explosive views of the exoskeleton were provided in Supplementary Figures S1-S3.

C. Subjects and Experimental Protocol

Eight male subjects (N = 8, age 24.75 ± 4.27 years, weight 76.31 ± 6.42 kg, height 178.50 ± 3.82 cm (mean ± SD)) participated in this experiment. All subjects were healthy and exhibited no gait abnormalities. The experimental protocol was approved by the Chinese Ethics Committee of Registering Clinical Trials (permit no. ChiECRCT20200232) and informed consents were obtained from all subjects. In the experiment, subjects walked on a treadmill at a normal speed of 1.25 m/s. No subject felt uncomfortable about the walking speed. The detailed experimental protocol was elucidated as follows.

The experimental protocol included two sessions: a habitual session and a testing session (Fig. 3). Each session was performed on a separated day to avoid fatigue effects. In all sessions, subjects walked on a treadmill at the speed of 1.25 m s^{-1} under five experimental conditions: one normal walking condition with no exoskeleton (NE), one walking with exoskeleton but with no assistance condition (NA), and three walking with exoskeleton assistance conditions (exoskeleton spring stiffness k = 5.25 (LOW), 8.5 (MED), 12 (HIGH) Nmm/deg). The stiffnesses of the spring were predefined to keep the assistive moment within the sensible limit

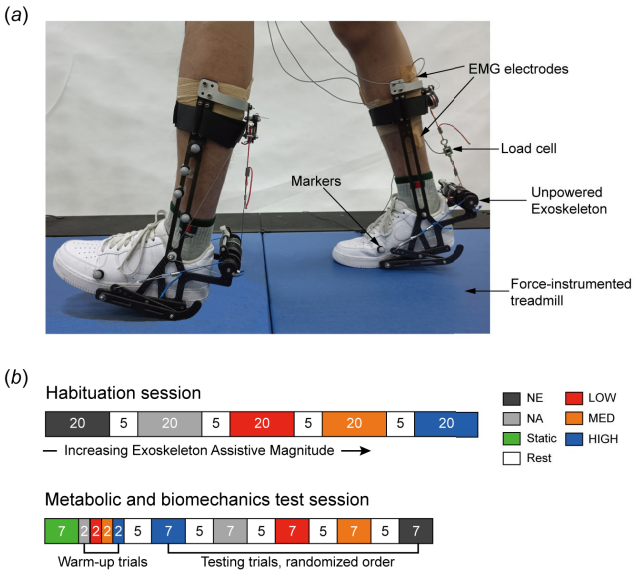

Fig. 3. Experiments of walking with the foot-ankle exoskeleton. (a). Participant wearing the unpowered foot-ankle exoskeleton. We used indirect calorimetry to measure metabolic rate, surface electromyography system to collect muscle activity and load transducers to record forces produced by the exoskeleton. In addition, reflective markers, motion capture system and force-instrumented treadmill were used to measure joint kinematics and kinetics. (b). Experimental Protocol. The number on the square represents the time duration (in minutes) of each trial. The colour of square indicates different walking conditions.

(see Supplementary Note S2 for the detailed explanation of the selection).

In the habitual session, subjects adapted themselves to each condition, and each habitual trial lasted 20 minutes. Subjects rested 5 minutes between each habitual trial. The habitual walking trials were in an increasing exoskeleton assistance magnitude order. In the testing session, subjects first performed a 7-minutes quiet standing trial for the measurement of basic metabolic rate. Then subjects underwent warm-up trials with different exoskeleton conditions, and each trial lasted for two minutes. After a 5-minute rest following the warm-up, the subjects began the formal test, which involved five 7-minutes test trials with different conditions: NE, NA, and three exoskeleton assistance conditions (LOW, MED, and HIGH). A 5-min break was given between each condition, and the order of conditions was randomized to minimize the ordering effect. We analyzed the data in the last 2 minutes of each trial to get the steady-state metabolic cost, joint kinematics, joint kinetics, exoskeleton mechanics, and lower limb muscle activities. The detailed methods of the measurements were stated in the next section.

D. Measurements and Data Analyses

The whole-body metabolic rates were measured via an indirect spirometry system (Jaeger Oxycon Mobile, CareFusion, Germany) according to a Brockway equation [36]. The respiratory exchange ratio (RER) was monitored throughout the experiments to ensure that the subjects were within the aerobic domain (RER $<$ 1) [37]. The net metabolic rate of each walking trial was calculated as the total metabolic rate minus the basic metabolic rate of quiet standing to reflect the energetic demands of walking. Then we normalized the net metabolic rate using body weight. Muscle activity (soleus, gastrocnemius, tibialis anterior, vastus lateralis, and semitendinous) were measured by an electromyography (EMG) system (SX230, Biometrics, Newport, UK, 1000 Hz). Electromyographic electrodes were attached to the right leg of the human body according to SEMINAM guidelines [38]. The EMG raw data was band-pass filtered (20–460 Hz) in the amplifier to retain the EMG signal content, then full-wave rectified and smoothed (fourth-order low-pass Butterworth filter, cut-off frequency 6 Hz) in the software (R2017a, Mathworks, USA) to get linear envelope [39], [40]. For standardized comparison across subjects, we normalized EMG data for each muscle using the maximum value observed during the NE condition.

Kinematic data were measured by a motion capture system (Vicon, Oxford, UK, 100 Hz). Retroreflective markers were attached to the lower limbs of subjects to record their motions. Specifically, markers were placed on the pelvis (four), and on the thigh (four), knee (two, only for the segment definitions), shank (four), ankle (two, only for the segment definitions), calcaneus (one), forefoot (two, distal heads of the first and fifth metatarsals) for each leg. The marker data were low-pass filtered at 6 Hz with a fourth-order Butterworth filter. Using the filtered marker data, we calculate the kinematics of step length, step width, and joint angles for hip, knee, and ankle of right leg through software (Visual3D, C-Motion, Germantown, MD, USA).

To measure kinetic data, we used a split-belt, force-instrumented treadmill (AMTI, Watertown, MA, USA, 1000 Hz) to record ground reaction force (GRF) during walking trails. The GRF data were low-pass filtered at 15 Hz with a fourth-order Butterworth filter. Combining GRF and marker data, the joint moment/power of hip, knee, and ankle of right leg were calculated via inverse dynamics using the software Visual3D (C-Motion, Germantown, MD, USA). Besides, we used a unified deformable segment analysis [34], [41] to calculate the beneath-hindfoot power of right leg, which was estimated as the power due to motion of the centre of mass (COM) of the foot relative to ground during the initial stance phase [27]. Note the beneath-hindfoot power included the power from both biological soft tissues beneath hindfoot and footwear, as well as the series element of the exoskeleton in the exoskeleton assistance conditions.

To estimate the exoskeleton's contribution to kinetics in the assistance conditions, we first measured the assistive force by a load cell (Forsentek, Shenzhen, China, 1000Hz) in series with the ankle rope of the right-side exoskeleton. The raw signals of load transducers were filtered with a Butterworth filter with a cut-off frequency of 15 Hz. Based on the measured assistive force, the exoskeleton moment and power at the ankle joint were calculated. Additionally, the exoskeleton's contribution to beneath-hindfoot work was calculated by subtracting the exoskeleton negative ankle work from the positive ankle work. Then the exoskeleton's contribution to beneath-hindfoot power was estimated by dividing the total beneath-hindfoot power by the ratio of exoskeleton's beneath-hindfoot work relative to total beneath-hindfoot work. The biological components of moment and power were obtained by subtracting corresponding exoskeleton moment/power from the total

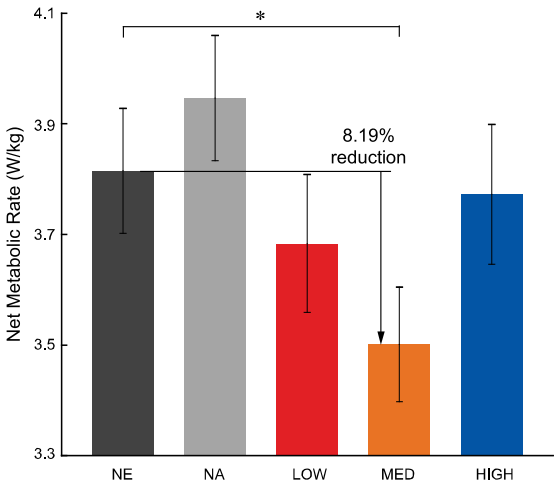

Fig. 4. Net metabolic rates during walking under different conditions. Among the five experiment conditions, walking with medium exoskeleton assistance (MED condition) shows the lowest net metabolic rate, and walking with exoskeleton but with no assistance (NA condition) consumes the highest metabolic rate. N = 8; bars, mean; error bars, s.e.m; Asterisks indicates significant difference compared to walking with no exoskeleton (NE condition) (two-sided paired t-test, $p < 0.05$).

moment/power respectively. The biological moment/power as well as exoskeleton moment/power were normalized using body weight.

To obtain the gait cycle average profiles of the biomechanical measurements for each trail, we broke the lower limb muscle activity, joint angles, joint moment/power, beneath-hindfoot power and exoskeleton assistive force into the gait cycle, which was defined by subsequent heel strikes of the right leg. Based on the average gait profiles of total moment/powers and exoskeleton assistive force, the biological and exoskeleton average gait profiles of moment/powers in the assistance conditions were then calculated. After obtaining the average gait profiles for each trail, these average curves for each condition were calculated by averaging across participants. The gait cycle average profiles provide intuitive representation for the time series of measured biomechanical data, while the individuated positive/negative portions of powers may be neutralized when averaging across participants. Consequently, we integrated the positive/negative portions of ankle and beneath-hindfoot power curves to calculate the corresponding work values of a gait cycle. Positive/negative average moments and powers were separated out using time integrals divided by corresponding positive/negative periods, respectively. Average magnitudes of muscle activity were calculated as their time integral divided by stride period in each condition for each participant. The peak values of biological and exoskeleton ankle positive moments/powers were also calculated considering their significance of push-off. Finally, the means and standard errors of the net metabolic rate, average moment, peak moment, average power, peak power, work per stride, average muscle activity, step length, step width and peak extension/flexion angle data were calculated across participants for each condition. These scalar quantities were then used to quantify the variation between different conditions utilizing further statistical analyses detailed below.

E. Statistical Analyses

We firstly used a two-sided goodness-of-fit test Jarque-Bera test to confirm that the net metabolic rate, average moment, peak moment, average power, peak power, ankle/foot work values of a gait cycle, average muscle activity, peak muscle activity, peak joint angle data and step length followed the normal distribution ($\alpha = 0.05$), which allowed us to conduct further statistical analyses. Then a mixed-model, two-way ANOVA (random effect: participant; fixed effects: exoskeleton assistive magnitude) was conducted on the above-mentioned metrics across conditions to determine the effect of assistive magnitude. The significance level was set at $\alpha = 0.05$. We also applied a two-sided paired t-test with Holm-Šidák correction on the above-mentioned metrics to compare exoskeleton conditions with no exoskeleton (NE) condition to find which exoskeleton condition showed a significant change. For the step width data that were not normally distributed, we instead used the Wilcoxon signed-rank, two-tailed test to compare exoskeleton conditions with no exoskeleton (NE) condition. All statistical analyses were performed via the software Matlab (R2017a, Mathworks, USA).

III. Results

A. Metabolic Rate

Across NE, NA, LOW, MED, and HIGH conditions, a two-factor, mixed-model ANOVA indicated a significant effect of exoskeleton assistive magnitude on net metabolic rate ($p < 0.01$). To be specific, with the increment of exoskeleton assistive magnitude, the metabolic rate first decreased then increased (Fig. 4). Compared to normal walking without exoskeleton, paired t-tests indicated the net metabolic rates were not significant different at NA (paired t-test: $p = 0.09$), LOW (paired t-test: $p = 0.07$) and HIGH conditions (paired t-test: $p = 0.66$), but showed 8.19 ± 0.96 % significant reduction at MED condition (paired t-test: $p < 0.01$). The detailed net metabolic rates for each subject are presented in Supplementary Table S2.

B. Exoskeleton Moment and Power

During the push-off phase, the average applied ankle moment and peak applied moment of the exoskeleton both increase with increasing assistive magnitude (Fig. 5d, mixed model two-way ANOVA: all $p < 0.01$). The positive ankle work and peak positive ankle power of exoskeleton both increased with increasing assistive magnitude (Fig. 5e, mixed model two-way ANOVA: all $p < 0.01$). The negative ankle work produced by exoskeleton first increased then remained unchanged with increasing assistive magnitude (mixed model two-way ANOVA: $p = 0.030$), while the peak negative ankle power of exoskeleton showed no significant changes with increasing assistive magnitude (mixed model two-way ANOVA: $p = 0.138$). Except for assisting the ankle joint, the exoskeleton also absorbs energy as the foot strike ground. During the heel-strike phase, the negative beneath-hindfoot work produced by the exoskeleton increased with increasing assistive magnitude (Fig. 5f, mixed model two-way ANOVA:

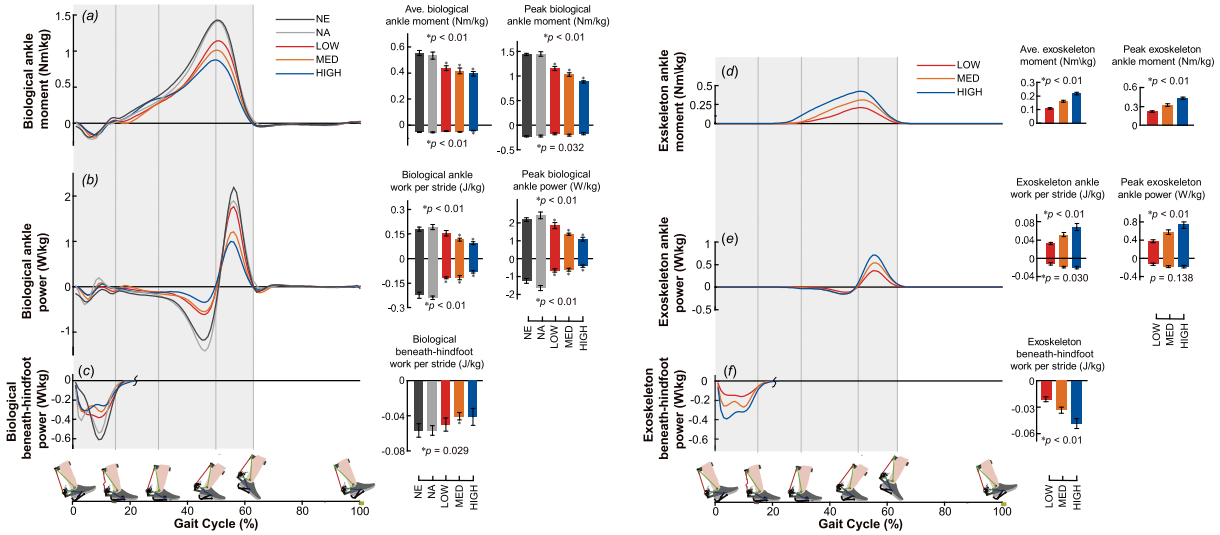

Fig. 5. Ankle and foot kinetics during walking under different conditions. (a-c) The biological moment curves and power curves, normalized to body weight for each condition, averaged across participants. The bar graphs on the right of the curves indicate the average biological moment, biological works, and peak biological ankle powers. (d-e) The exoskeleton moment curves and power curves, normalized to body weight for each condition, averaged across participants. The bar graphs on the right of the curves indicate the average exoskeleton moment, exoskeleton works, and peak exoskeleton ankle powers. Positive values represent biological and exoskeleton ankle plantarflexion moments. N = 8; error bars, s.e.m; p values are the results of mixed model two-way ANOVA (random effect: participant; fixed effect: assistive magnitude). Asterisks on the error bar indicate significant differences compared to walking with no exoskeleton (NE condition) (two-sided paired t-test, $p < 0.05$). Ave., average.

$p < 0.01$). The detailed kinetical parameters of the exoskeleton are presented in Supplementary Table S3.

C. Kinetics and Muscle Activity

With the energy modulation of the exoskeleton, the average biological ankle joint plantarflexion moment, biological ankle joint work, peak biological ankle joint plantarflexion moment, peak biological ankle joint positive power and peak biological ankle joint negative power were all reduced (mixed model two-way ANOVA: all $p < 0.01$). In addition, the biological beneath-hindfoot work was also reduced with the exoskeleton assistance (mixed model two-way ANOVA: $p = 0.029$). As shown in Fig. 5a-c, the biological ankle joint moments and powers mainly decreased during the push-off phase, while the biological beneath-hindfoot power mainly decreased during the heel-strike phase, in agreement with the assistive interval of the exoskeleton (Fig. 5d-f). The detailed kinetical parameters are presented in Supplementary Table S4.

The mean activities of measured skeletal muscles also showed significant changes across different conditions (Fig. 6, mixed model two-way ANOVA: all $p < 0.05$). Under MED condition, the average activities of target soleus, gastrocnemius and vastus lateralis decreased by 9.34 %, 8.91 % and 10.17 % compared to NE condition (paired t-test: $p < 0.01$, $p < 0.01$ and $p = 0.021$), without adding the average activity of tibialis anterior and semitendinous (paired t-test: $p = 0.646$ and $p = 0.348$). However, the HIGH condition was found to increase the average tibialis anterior activity and average semitendinous activity (paired t-test: $p = 0.030$ and $p = 0.046$). The changes of peak activities of measured skeletal muscles across conditions were not significant (Fig. 6, mixed model two-way ANOVA: $p > 0.05$), except for tibialis anterior and vastus lateralis (Fig. 6, mixed model two-way ANOVA: $p = 0.016$ and $p = 0.003$). Under MED condition, the peak

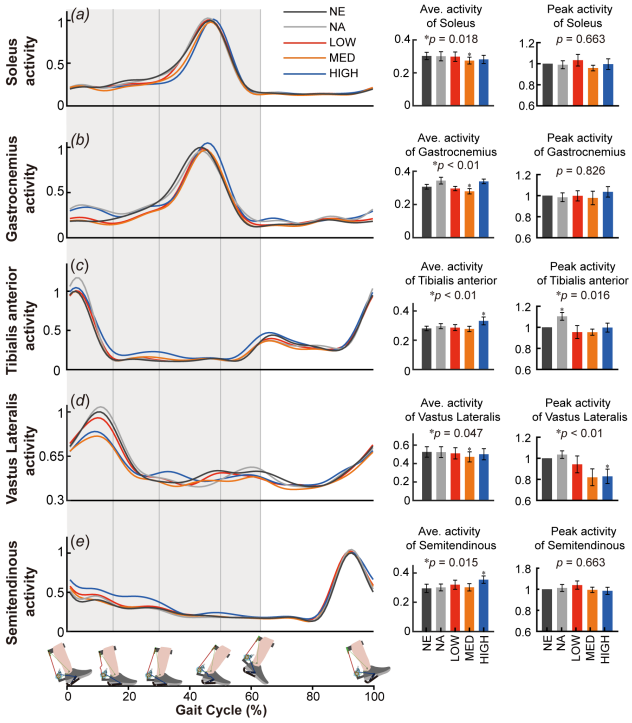

Fig. 6. Muscle activities during walking under different conditions. (a) Soleus (b) Gastrocnemius (c) Tibialis anterior (d) Vastus lateralis (e) Semitendinosus. All values were averaged across participants and normalized to the maximum value in no exoskeleton condition (NE). Bar graphs on the right are the average and peak muscle activity over the whole gait cycle for each condition. N = 8; bars, mean; error bars, s.e.m; p values are the results of mixed model two-way ANOVA (random effect: participant; fixed effect: assistive magnitude). Asterisks on the error bar indicate significant differences compared to NE condition (two-sided paired t-test, $p < 0.05$). Ave., average.

activity of vastus lateralis decreased by 18.04% compared to NE condition (paired t-test: $p = 0.058$). Peak soleus and gastrocnemius activities during terminal stance decreased for

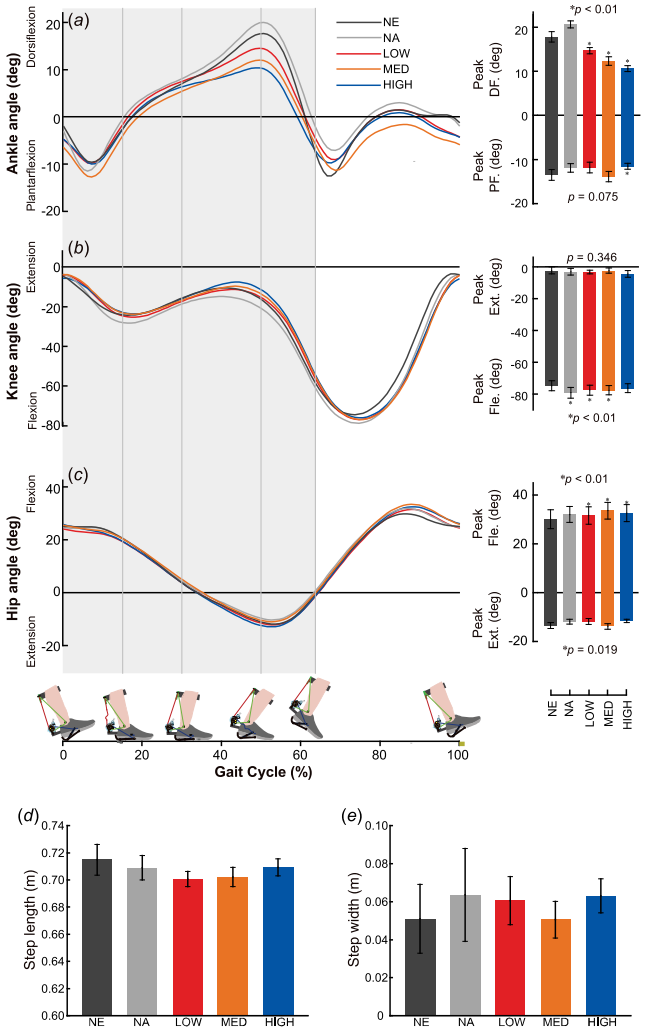

Fig. 7. Kinematics during walking under different conditions. The joint angles of (a) ankle, (b) knee and (c) hip over the gait cycle, averaged across participants. The bar graphs on the right are the range of motion for each joint and each condition. (d) step length and (e) step width, averaged across gait cycle and participants. N = 8; bars, mean; error bars, s.e.m; p values are the results of mixed-model two-way ANOVA (random effect: participant; fixed effect: assistive magnitude). Asterisks on the error bar indicate significant differences compared to NE condition (two-sided paired t-test, p < 0.05). Ave., average; DF., dorsiflexion; PF. plantarflexion; Ext., extension; Flex., flexion.

the MED condition by 2.18 % and 4.13 % compared to NE condition, but the changes were not significant (paired t-test: $p = 0.164$ and $p = 0.742$). The detailed muscle activity parameters are presented in Supplementary Table S4.

D. Kinematics

As shown in Fig. 7a-c, except the peak ankle plantarflexion angle and peak knee extension angle remained unchanged (mixed model two-way ANOVA: $p = 0.075$ and $p = 0.346$), the other peak joint angles all showed significant differences across different conditions (mixed model two-way ANOVA: all $p < 0.05$). For the MED condition which showed significant metabolic rate reduction, the peak ankle dorsiflexion angle decreased (paired t-test: $p < 0.01$), the peak knee flexion increased (paired t-test: $p = 0.025$), the peak hip flexion angle increased (paired t-test: $p < 0.01$) compared to NE condition. The step length for the MED condition decreased by 1.80% compared to NE condition, but the changes were not significant (Fig. 7d, paired t-test: $p = 0.152$). The change of step width for MED condition was also not significant compared to NE condition (Fig. 7e, Wilcoxon signed-rank test, two-tailed, $p = 0.188$). The detailed kinematical parameters are presented in Supplementary table S5.

IV. Discussion

We have demonstrated that the walking economy can be improved by developing an effective energy loop between the foot and ankle joint using an unpowered exoskeleton. Unlike previous passive exoskeletons recycled energy from lower limb joints [22], [23], [42], our result demonstrated that storing and transferring energy from the heel-strike collision is a viable method for providing an energy source of walking assistance. By modulating energy among the foot-ankle complex effectively, the net metabolic rate was significantly reduced by 8.19 ± 0.96 % compared to normal walking without the exoskeleton (Fig. 4).

The skeletal muscle is the primary consumers of metabolic energy during walking [43]. The direct reason for the metabolic cost reduction may be the significant reduction in muscle activity of ankle plantarflexors during mid-stance and quadriceps during initial stance (Fig. 6). While previous studies have found that the cushion of heel-strike can enhance running economy [35], [44], the cushion in walking activities draws little attention due to the much less collision of walking compared to running. Our results provided new insight into the human response to cushion assistance during walking. As shown in Fig. 5c and Fig. 6d, the added cushion beneath the hindfoot can also improve the walking economy by offloading the biological efforts to decelerate the foot as the heel striking ground. Furthermore, our results indicated no increase in antagonist tibialis anterior and semitendinous co-contractions in LOW and MED conditions (Fig. 6), suggesting the exoskeleton may enhance walking economy in a natural manner that exoskeleton did not interfere with subjects. In addition, no significant differences of step length and step width were found between normal walking condition and walking with exoskeleton conditions, which also indicate that the exoskeleton did not break human natural walking. Nevertheless, the joint angles of the subjects significantly changed with the assistance of the exoskeleton (Fig. 7). Previous experimental and theoretical studies have found humans prefer to walk in ways that optimize energetic cost [45], [46]. Although we cannot affirm from this study, the kinematic changes may be a result of subjects' adaption to the exoskeleton assistance for walking economy.

Excessive assistance magnitude of exoskeleton under the HIGH condition instead resulted in less metabolic benefit (Fig. 4). The high assistive ankle moment significantly decreased the dorsiflexion motion of the ankle joint during the mid-late stance phase (Fig. 7), which impairs the positive rotation of the energy axle of the exoskeleton to release the stored energy. To ensure the complete working process of the exoskeleton, we slightly tensioned the ankle rope under

HIGH condition, which lead to the early timing of applying ankle assistive moment (Fig. 5d). This shift resulted in that assistive ankle moment was exerted before the mid-stance phase. Previous studies have found the externally applied ankle moment in early stance caused increasing activation of ankle dorsiflexors and hamstrings [22], [26], which was also observed in our results (Fig. 6). Besides, the shifted timing also impaired the impulsive trend of ankle assistive moment in late stance, accompanied by the increase of ankle plantarflexor activity. Future work using ultrasound imaging may give further explanations from the aspect of neuromuscular factors [47]. In turn, these negative effects in HIGH condition could also imply the importance of the timing and manner of releasing energy on the ankle joint to the walking economy.

Although the experimental results indicate that wearing the developed exoskeleton can reduce the metabolic cost of walking, we acknowledge that there are still a number of limitations to this study. First, the striking rod sinks below the shoe by about 2.5 cm to allow the exoskeleton to collect heel-strike energy. Although the foot has a natural clearance of 1-2 cm between heel and ground during the swing phase of normal walking [48], [49], it seemed the subjects still lifted their feet slightly to avoid the curved bar banging into ground during the swing phase of walking with exoskeleton. According to our results (Fig. 7a-c), when subjects walked with the exoskeleton, their peak knee flexion angle and peak hip flexion angle during the mid-swing phase both increased slightly compared to normal walking, which may account for the increased metabolic cost of wearing exoskeleton but with no assistance. This phenomenon may be improved by optimizing the geometrical shapes of the striking rod in future works. Second, the foot frames of the exoskeleton have the protrusions posterior to human foot, which may interfere with some daily activities, such as stepping off curbs or down stairs. The interferences caused by the protrusions may impede societal adoption of the exoskeleton [50]. Future iteration design could reduce the protruding structures of the developed exoskeleton for more fitting form. Finally, the peak activations of ankle plantarflexors showed little variation during the terminal stance phase of different conditions, which was unexpected as the peak values of biological ankle moment and power during the terminal phase were significantly reduced by exoskeleton assistance. This phenomenon may be due to the exoskeleton assistance altered the muscle contractile length and velocity to unfavorable states [51], [52] during terminal stance. Deeper insight about the muscle contractile mechanism could be obtained by adopting approaches of ultrasound imaging experiment [47] or musculotendon mechanics modeling [53], based on which our exoskeleton design may be improved for more metabolic cost reduction of walking.

V. Conclusion

Here, we have proved how the developed energy loop between the foot and ankle joint can improve the walking economy without any external energy input. By reasoning energy modulation strategy from energy flow characteristics of human walking and building exoskeleton relied on the passive mechanical mechanism, the metabolic cost of human walking was reduced in a natural manner. With medium exoskeleton assistance, the average activities of target ankle plantarflexors and quadriceps were significantly reduced without adding the muscular burden of the antagonists. While the peak values of biological ankle moment and power during the terminal phase were significantly reduced by exoskeleton assistance, it was unexpected that the peak activations of ankle plantarflexors during the terminal stance were not significantly altered. On the basis of the energy modulation strategy and experimental results presented here, future works could improve the mechanical mechanism of the exoskeleton to enable larger assistive magnitude or more suitable assistive timing to further reduce the peak activations of ankle plantarflexors for better enhancement of walking economy. Rather than emulating or strengthening the functions of existing biological structures, developing a complementary energy loop that does not exist in the human body itself may point out a new direction for future research in the unpowered exoskeleton and gait assistance.

References

[1] D. A. Winter, *Biomechanics and Motor Control of Human Movement*. 4th ed. Hoboken, NJ, USA: Wiley, 2009.

[2] M. H. Dickinson, C. T. Farley, R. J. Full, M. A. R. Koehl, R. Kram, and S. Lehman, "How animals move: An integrative view," *Science*, vol. 288, no. 5463, pp. 100–106, Apr. 2000.

[3] D. J. Farris, L. A. Kelly, A. G. Cresswell, and G. A. Lichtwark, "The functional importance of human foot muscles for bipedal locomotion," *Proc. Nat. Acad. Sci. USA*, vol. 116, no. 5, p. 1645, Jan. 2019.

[4] K. Z. Takahashi and S. J. Stanhope, "Mechanical energy profiles of the combined ankle–foot system in normal gait: Insights for prosthetic designs," *Gait Posture*, vol. 38, no. 4, pp. 818–823, Sep. 2013.

[5] D. J. Farris and G. S. Sawicki, "The mechanics and energetics of human walking and running: A joint level perspective," *J. Roy. Soc. Interface*, vol. 9, no. 66, pp. 110–118, Jan. 2012.

[6] K. E. Zelik and P. G. Adamczyk, "A unified perspective on ankle push-off in human walking," *J. Exp. Biol.*, vol. 219, no. 23, p. 3676, Dec. 2016.

[7] G. S. Sawicki, C. L. Lewis, and D. P. Ferris, "It pays to have a spring in your step," *Exerc. Sport Sci. Rev.*, vol. 37, no. 3, pp. 130–138, Jul. 2009.

[8] K. T. Bates *et al.*, "The evolution of compliance in the human lateral mid-foot," *Proc. Roy. Soc. B, Biol. Sci.*, vol. 280, no. 1769, Oct. 2013, Art. no. 20131818.

[9] K. Deschamps, M. Eerdekens, E. Monbaliu, G. Gijon, and F. Staes, "Biomechanical maturation of foot joints in typically developing boys: Novel insight in mechanics and energetics from a cross-sectional study," *Gait Posture*, vol. 85, pp. 244–250, Mar. 2021.

[10] H. Pontzer, "Economy and endurance in human evolution," *Current Biol.*, vol. 27, no. 12, pp. R613–R621, Jun. 2017.

[11] D. P. Ferris, G. S. Sawicki, and M. A. Daley, "A physiologist's perspective on robotic exoskeletons for human locomotion," *Int. J. Humanoid Robot.*, vol. 4, no. 3, pp. 507–528, Sep. 2007.

[12] A. J. Young and D. P. Ferris, "State of the art and future directions for lower limb robotic exoskeletons," *IEEE Trans. Neural Syst. Rehabil. Eng.*, vol. 25, no. 2, pp. 171–182, Feb. 2017.

[13] H. Herr, "Exoskeletons and orthoses: Classification, design challenges and future directions," *J. NeuroEng. Rehabil.*, vol. 6, no. 1, p. 21, Jun. 2009.

[14] G. S. Sawicki, O. N. Beck, I. Kang, and A. J. Young, "The exoskeleton expansion: Improving walking and running economy," *J. Neuroeng. Rehabil.*, vol. 17, no. 1, p. 25, Feb. 2020.

[15] L. M. Mooney, E. J. Rouse, and H. M. Herr, "Autonomous exoskeleton reduces metabolic cost of human walking," *J. Neuroeng. Rehabil.*, vol. 11, no. 1, p. 151, Nov. 2014.

[16] R. W. Nuckols, S. Lee, K. Swaminathan, D. Orzel, R. D. Howe, and C. J. Walsh, "Individualization of exosuit assistance based on measured muscle dynamics during versatile walking," *Sci. Robot.*, vol. 6, no. 60, Nov. 2021, Art. no. eabj1362.

[17] G. S. Sawicki and D. P. Ferris, "Powered ankle exoskeletons reveal the metabolic cost of plantar flexor mechanical work during walking with longer steps at constant step frequency," *J. Exp. Biol.*, vol. 212, no. 1, pp. 21–31, 2009.

[18] R. W. Jackson and S. H. Collins, "An experimental comparison of the relative benefits of work and torque assistance in ankle exoskeletons," *J. Appl. Physiol.*, vol. 119, no. 5, pp. 541–557, 2015.

[19] J. Zhang *et al.*, "Human-in-the-loop optimization of exoskeleton assistance during walking," *Science*, vol. 356, no. 6344, p. 1280, Jun. 2017.

[20] H. Han *et al.*, "Selection of muscle-activity-based cost function in human-in-the-loop optimization of multi-gait ankle exoskeleton assistance," *IEEE Trans. Neural Syst. Rehabil. Eng.*, vol. 29, pp. 944–952, 2021.

[21] T. G. Sugar, K. W. Hollander, A. Boehler, and J. Ward, "Comparison and analysis of a robotic tendon and jackspring actuator for wearable robotic systems," *J. Med. Devices*, vol. 7, no. 4, Sep. 2013.

[22] S. H. Collins, M. B. Wiggin, and G. S. Sawicki, "Reducing the energy cost of human walking using an unpowered exoskeleton," *Nature*, vol. 522, no. 7555, pp. 212–215, 2015.

[23] E. Etenzi, R. Borzuola, and A. M. Grabowski, "Passive-elastic knee-ankle exoskeleton reduces the metabolic cost of walking," *J. Neuroeng. Rehabil.*, vol. 17, no. 1, p. 104, Jul. 2020.

[24] Y. Chang, W. Wang, and C. Fu, "A lower limb exoskeleton recycling energy from knee and ankle joints to assist push-off," *J. Mech. Robot.*, vol. 12, no. 5, Apr. 2020, Art. no. 051011.

[25] T. Zhou, C. Xiong, J. Zhang, W. Chen, and X. Huang, "Regulating metabolic energy among joints during human walking using a multiarticular unpowered exoskeleton," *IEEE Trans. Neural Syst. Rehabil. Eng.*, vol. 29, pp. 662–672, 2021.

[26] R. W. Nuckols and G. S. Sawicki, "Impact of elastic ankle exoskeleton stiffness on neuromechanics and energetics of human walking across multiple speeds," *J. Neuroeng. Rehabil.*, vol. 17, no. 1, p. 75, Jun. 2020.

[27] E. C. Honert and K. E. Zelik, "Foot and shoe responsible for majority of soft tissue work in early stance of walking," *Hum. Movement Sci.*, vol. 64, no. 1, pp. 191–202, Apr. 2019.

[28] S. H. Collins and A. D. Kuo, "Recycling energy to restore impaired ankle function during human walking," *PLoS ONE*, vol. 5, no. 2, p. e9307, Feb. 2010.

[29] K. E. Zelik *et al.*, "Systematic variation of prosthetic foot spring affects center-of-mass mechanics and metabolic cost during walking," *IEEE Trans. Neural Syst. Rehabil. Eng.*, vol. 19, no. 4, pp. 411–419, Aug. 2011.

[30] J. J. Collins and M. W. Whittle, "Impulsive forces during walking and their clinical implications," *Clin. Biomech.*, vol. 4, no. 3, pp. 179–187, Aug. 1989.

[31] M. W. Whittle, "Generation and attenuation of transient impulsive forces beneath the foot: A review," *Gait Posture*, vol. 10, no. 3, pp. 264–275, Dec. 1999.

[32] K. Z. Takahashi, K. Worster, and D. A. Bruening, "Energy neutral: The human foot and ankle subsections combine to produce near zero net mechanical work during walking," *Sci. Rep.*, vol. 7, no. 1, p. 15404, Nov. 2017.

[33] S. Lipfert, M. Günther, D. Renjewski, and A. Seyfarth, "Impulsive ankle push-off powers leg swing in human walking," *J. Exp. Biol.*, vol. 217, no. 8, p. 1218, Jan. 2013.

[34] K. E. Zelik and E. C. Honert, "Ankle and foot power in gait analysis: Implications for science, technology and clinical assessment," *J. Biomech.*, vol. 75, no. 1, pp. 1–12, Jun. 2018.

[35] K. D. Tung, J. R. Franz, and R. Kram, "A test of the metabolic cost of cushioning hypothesis during unshod and shod running," *Med. Sci. Sports Exerc.*, vol. 46, no. 2, pp. 324–329, Feb. 2014.

[36] J. M. Brockway, "Derivation of formulae used to calculate energy expenditure in man," *Hum. Nutrition Clin. Nutrition*, vol. 41, no. 6, pp. 463–471, 1987.

[37] G. A. Brooks, T. D. Fahey, and T. P. White, *Exercise Physiology: Human Bioenergetics and Its Applications*, 1 ed. Menlo Park, CA, USA: Mayfield, 1996.

[38] H. J. Hermens *et al.*, "European recommendations for surface electromyography," *Roessingh Res. Dev.*, vol. 8, no. 2, pp. 13–54, 1999.

[39] D. A. Winter, "Kinesiological electromyography," in *Biomechanics and Motor Control of Human Movement*, D. A. Winter, Ed. Hoboken, NJ, USA: Wiley, 2009, ch. 10.

[40] R. Merletti and P. Di Torino, "Standards for reporting EMG data," *J. Electromyogr. Kinesiol.*, vol. 9, no. 1, pp. 3–4, 1999.

[41] K. Z. Takahashi, T. M. Kepple, and S. J. Stanhope, "A unified deformable (UD) segment model for quantifying total power of anatomical and prosthetic below-knee structures during stance in gait," *J. Biomech.*, vol. 45, no. 15, pp. 2662–2667, Oct. 2012.

[42] T. Zhou, C. Xiong, J. Zhang, D. Hu, W. Chen, and X. Huang, "Reducing the metabolic energy of walking and running using an unpowered hip exoskeleton," *J. Neuroeng. Rehabil.*, vol. 18, no. 1, p. 95, Jun. 2021.

[43] M. J. Joyner and D. P. Casey, "Regulation of increased blood flow (Hyperemia) to muscles during exercise: A hierarchy of competing physiological needs," *Physiol. Rev.*, vol. 95, no. 2, pp. 549–601, Apr. 2015.

[44] W. Hoogkamer, R. Kram, and C. J. Arellano, "How biomechanical improvements in running economy could break the 2-hour Marathon barrier," *Sports Med.*, vol. 47, no. 9, pp. 1739–1750, Sep. 2017.

[45] J. C. Selinger, S. M. O'Connor, J. D. Wong, and J. M. Donelan, "Humans can continuously optimize energetic cost during walking," *Current Biol.*, vol. 25, no. 18, pp. 2452–2456, 2015.

[46] M. Srinivasan and A. Ruina, "Computer optimization of a minimal biped model discovers walking and running," *Nature*, vol. 439, pp. 72–75, Sep. 2005.

[47] R. W. Nuckols, T. J. M. Dick, O. N. Beck, and G. S. Sawicki, "Ultrasound imaging links soleus muscle neuromechanics and energetics during human walking with elastic ankle exoskeletons," *Sci. Rep.*, vol. 10, no. 1, p. 3604, Feb. 2020.

[48] B. Mariani, S. Rochat, C. J. Büla, and K. Aminian, "Heel and toe clearance estimation for gait analysis using wireless inertial sensors," *IEEE Trans. Biomed. Eng.*, vol. 59, no. 11, pp. 3162–3168, Nov. 2012.

[49] A. R. Wu and A. D. Kuo, "Determinants of preferred ground clearance during swing phase of human walking," *J. Exp. Biol.*, vol. 219, no. 19, p. 3106, Jan. 2016.

[50] M. B. Yandell, J. R. Tacca, and K. E. Zelik, "Design of a low profile, unpowered ankle exoskeleton that fits under clothes: Overcoming practical barriers to widespread societal adoption," *IEEE Trans. Neural Syst. Rehabil. Eng.*, vol. 27, no. 4, pp. 712–723, Apr. 2019.

[51] B. R. MacIntosh, "Recent developments in understanding the length dependence of contractile response of skeletal muscle," *Eur. J. Appl. Physiol.*, vol. 117, no. 6, pp. 1059–1071, Jun. 2017.

[52] J. Alcazar, R. Csapo, I. Ara, and L. M. Alegre, "On the shape of the force-velocity relationship in skeletal muscles: The linear, the hyperbolic, and the double-hyperbolic," *Frontiers Physiol.*, vol. 10, p. 769, Jun. 2019.

[53] R. W. Jackson, C. L. Dembia, S. L. Delp, and S. H. Collins, "Muscle-tendon mechanics explain unexpected effects of exoskeleton assistance on metabolic rate during walking," *J. Exp. Biol.*, vol. 220, no. 11, pp. 2082–2095, Jan. 2017.